Numerical Investigation of Liquefaction Potential in Sabkha Soil Supporting Foundation Subjected to Vibration Loading

DOI : 10.36909/jer.18597

Naif Alsanabani*, Ahmed Alnuaim*

*Department. of Civil Engineering, Engineering College, King Saud University, Riyadh, 11421, Saudi Arabia

Corresponding author E-mail: alnuaim@ksu.edu.sa

Abstract

Liquefaction is a major concern, especially in loose soil subjected to vibrations, which may lead to severe damage to buildings and infrastructure. In this paper, the influence of vertical vibrational loading on the liquefaction potential of natural sabkha soil was numerically examined to understand the effects of different parameters, on liquefaction potential. The parameters considered in this study include vertical displacement amplitude, frequency, modified mass ratio, subsoil conditions (natural and cement-stabilized sabkha soil with 5% and 10% cement content), and thickness ratio of cement-stabilized sabkha soil. Liquefaction was observed for different foundation configurations. The pore water pressure ratio beneath the foundation increased with a decrease in foundation mass. The minimum foundation mass that prevents liquefaction in the sabkha soil depends on the ratio of the machine's velocity to the shear wave velocity of the subsoil (sabkha). The study provides guidance and information on the risk of constructing a foundation that is subjected to continuous vibration (such as the foundations of machines) in saturated sabkha soils due to the low rigidity, resulting from the generation of pore water pressure during the dynamic loading.

Keywords: sabkha; pore water pressure; liquefaction; vibration

Introduction

Liquefaction is a major problem in geotechnical engineering, especially under seismic and dynamic loading. It causes different failure damages to slopes, infrastructure, retaining walls, and foundations (Kramer, 1996). Liquefaction is a condition where pore water pressure (PWP) in cohesionless soil builds up to a level where the effective stress becomes zero, and the soil loses its strength. Initial liquefaction corresponds to the condition when PWP equals the confining pressure σ_3. In most cases, 20% double amplitude strain is considered a failure. Cyclic mobility is a liquefaction phenomenon triggered by cyclic loading occurring in soil deposits with static shear stresses lower than the soil strength. Experimental and numerical studies on the liquefaction behavior of different soil types supporting foundations and subjected to dynamic loading have been reported (Amini and Qi, 2000; El Fiky et al., 2020; Ibrahim, 2014; Lee, 2007; Mokhtar et al., 2014; Rollins and Seed, 1990; Vaid and Thomas, 1995; Yoshimi, 1967; Zeghal and Elgamal, 1994). Their main results showed that liquefaction depends on the resistance of sand to deformation, and the applied shear stress can reduce the volume or collapse the structure. Liquefaction also depends on the fabrics of sand, including gradation, particle size and shape, relative density, confining pressure, and initial stress state. Irregular cyclic loading due to earthquakes is the most common cause of dynamic liquefaction.

In order to understand the liquefaction potential of sabkha soil, it is important to know the basics of the soil. Sabkha has poor to medium density. It is considered problematic soil and has liquefaction potential (Ahmed and Al Shayea, 2017). Sabkha soil is widespread in coastal semi-arid regions, such as the Eastern and Western regions of Saudi Arabia. Some regions where sabkha soil is found witness a rapid increase in development, urbanization, and industrial activities. Some factories in such regions have reciprocating and centrifugal machines that need adequate support

systems due to the high vibration induced by the machines. Machine foundations should satisfy dynamic requirements, which depend on the dynamic properties of subsoil and the dynamic loading characteristics. Sabkha soil is not instantaneously collapsible and requires a sufficient volume of water to dissolve cementing agents, making them unsuitable for infrastructural support (Al-Amoudi and Abduljauwad, 1994, 1995; Al-Shamrani, 2004; Al-Shamrani and Dhowian, 1996). Ahmed and Al Shayea, 2017 studied the liquefaction potential of sabkha soil under seismic loading and stated that the loose soil layers cannot be liquefied for peak horizontal acceleration of more than 0.035 g. However, liquefaction is anticipated at higher PHA (Peak Horizontal Acceleration) values (0.055, 0.07, 0.08, and 0.10 g) for subsurface profiles/zones with corresponding thicknesses of 6, 4, 3, and 2 m for loose sandy sabkha soil layers.

Among these studies, the liquefaction behavior of sabkha soil under vibrational loading has not been reported. Thus, in this study, the liquefaction of sabkha soil supporting foundations subjected to vertical vibration was numerically studied by examining the excess PWP of points underneath foundations at different displacement amplitudes and operating frequencies. The sinusoidal displacement amplitude that was applied on the foundation varied from 0.004, 0.04, and 0.0.4 mm and the operation frequency was 5, 20, and 80 Hz. The influence of foundation mass that was subjected to vertical vibration on the liquefaction behavior of natural sabkha was examined by varying the modified mass ratio (based on Eq. 5) as 0.012, 0.053, 0.15, and 0.06.

NATURAL SABKHA SOIL PROPERTIES

It is necessary to evaluate the properties of sabkha soil used in numerical modeling. To evaluate the properties of the sabkha soil, samples were collected from Ras Al-Ghar in Eastern Saudi Arabia. The field density, water content, sieve analysis, hydrometer analysis, Atterberg limits, and specific gravity of sabkha soil have been investigated according to ASTM standards

(ASTM D2216-10, 2010; ASTM D422, 2007; ASTM D4318-10, 2010; ASTM D6938–10, 2010; ASTM D854, 2010). Their results with the results of mineralogy tests can be referred to in (Alnuaim et al., 2021). The general properties of the soil are shown in Table 1.

Table 1 Properties and classification of the sabkha soil (Alsanabani, 2021).

Property	Value
Specific gravity, Gs	2.78
Passing through # 200 (%)	27.74
Effective size, D_{10} (mm)	0.02
***D_{30} (mm)**	0.09
****D_{60} (mm)**	0.21
Coefficient of uniform, C_u	11.39
Coefficient of curvature, C_c	2.20
USCS Soil type	SM
AASHTO soil type	A-3

*D_{30} is the size at which 30% is finer by weight.

**D_{60} is the size at which 60% is finer by weight.

FINITE ELEMENT METHOD (FEM) MODELING

The FEM procedures consist of preprocessing, processing, and postprocessing stages. The preprocessing stage compromises the setting of meshing issues (element size, time size, boundary conditions that depend on the characteristics of dynamic loading (magnitude, frequency, phase angle) and selecting the appropriate constitutive model. In the processing stage, consider the select type of analysis (static, consolidation, dynamic), drain, or undrained condition. The postprocessing stage, in the final, displays the output results in terms of kinematic (displacement, strain, strain

rate) and kinetic (normal and tangential of the total or effective stresses, pore water pressure). More details of the stages are in the following sections. The governing equation used in dynamic analysis represents three components as; inertia force ($m\ddot{u}$), damping force ($c\dot{u}$), and stiffness force (Ku), it can be represented in Eq. (1) as;

$$m\ddot{u} + c\dot{u} + Ku = F(t) \quad (1)$$

where $\ddot{u}$, $\dot{u}$, and u are acceleration, velocity, and displacement vectors, respectively, m is a mass matrix, c is the damping matrix, K is the stiffness matrix, F(t) is the external dynamic load vector that varies with time (t). the stiffness matrix depends on the constitutive model of the foundation material and subsoil (sabkha), where the capture of the decreasing stiffness of the saturated sabkha due to increasing the pore water pressure throughout dynamic loading (at the undrained condition) should be considered by selecting an appropriate constitutive model such as UBC3D-PLM.

The liquefaction potential of saturated sabkha soil was numerically investigated using PLAXIS 3D. The system consists of a subsoil (natural sabkha) and a circular foundation subjected to sinusoidal cyclic vertical displacement amplitude for frequencies of 5, 20, and 80 Hz. Due to the rapid cyclic loading, the sabkha was analyzed with the undrained condition. The foundation's diameter was kept constant at 5 m. To eliminate boundary effects on the results of the FEM, the FEM domain was 6 times the dimensions of the structure, as recommended by Bhatia (Bhatia, 2008). The analysis performed herein is a quasi-static system; thus, the horizontal dimensions of the domain are 10 times the foundation diameter, and viscous boundary conditions were employed to eliminate the influence of reflected waves. The relaxation coefficients for normal and tangential boundary conditions were set as 1.0 and 0.25, respectively (standard values) (MUÑOZ, 2008.)

Three elements were used in the analysis: (1) 10-node tetrahedral elements to simulate sabkha and cement-stabilized sabkha soil; (2) 6-node triangle plate elements to simulate foundations; (3) 6-node elements to simulate structure–soil interfaces. Notably, one-quarter of the system was considered to reduce calculation time. The size of elements affects the accuracy of FEM analysis, and it depends on the wavelength transmitted through the element. Large or coarse elements may infiltrate the transmitted wave: the size of elements should be $\frac{1}{5}$ to $\frac{1}{8}$ of the wavelength (λ) (Kramer, 1996), which can be calculated based on the velocity (v) (compressive or shear) and frequency (f) using ($\lambda = vf$). The shear wave velocity for sabkha samples was measured using the bender element, and it was 85, 120, and 211 m/s for effective confining stress of 50, 100, and 150 kPa, respectively (Alnuaim et al., 2020). Operation frequencies of 5, 20, and 80 Hz were considered in the FEM analysis; therefore, the lower bound of the element size was approximately 0.3 m.

For wave propagation, the time step should be considered small so that the wave does not travel more than the element length in each step; otherwise, the results will be unreliable. The time step depends on the wavelength for the highest velocity, which is the p-wave. According to (Bhatia, 2008) and (Bathe, 2006), the maximum time step size used is given as ($\Delta t_{increment} = \frac{L_{ele}}{v_s}$) where L_{ele} is the element length, and v_s is the shear wave velocity.

Constitutive model

UBC3D-PLM was used to model sabkha soil under cyclic loading to evaluate the liquefaction potential. The UBC3D-PLM model adopts elastic-plastic behavior with plastic hardening and can assess the increase in excess PWP in undrained conditions or the increase in

densification in drained conditions under dynamic loading, as expressed in Eq. (1) (Petalas & Galavi, 2013) as;

$$K^{p}_{G,secondary} = K^{P}_{G}\left(4 + \frac{n_{rev}}{2}\right) hard\ f_{dens} \quad (1)$$

where $K_{G,secondary}$, and K^{P}_{G} are the secondary and input plastic shear modulus factors, respectively, n_{rev} is the number of shear stress reversals from loading to unloading, f_{dens} is a multiplier factor (a user input parameter to adjust the densification rule), and *hard* is a factor which is correcting the densification factor for loose soil, and it is expressed by Eq. (2) (Petalas & Galavi, 2013);

$$hard = min\left(1, max\ (0.5, 0.1N_{60})\right) \quad (2)$$

where N_{60} is the corrected SPT value.

Under undrained conditions, excess PWP can be computed based on the bulk modulus of water (*Kw*), which varies with step. K_w is calculated based on soil porosity (*n*), undrained bulk modulus (K_u), and effective bulk modulus (K'), which depends on the plastic shear modulus number (K^{p}_{G}) (Petalas & Galavi, 2013). Saturated sabkha soil was modeled using UBC3D-PLM to consider the effect of the generated excess PWP under vertical vibration loading. The parameters used in UBC3D-PLM are categorized into stiffness, strength, and densification parameters. In terms of stiffness, it is stress-dependent and increases with depth. The stiffness parameters for UBC3D-PLM include K^{e}_{B}, $K^{e}_{G}, K^{p}_{G}, ne, me, and\ np$, which vary with depth. The strength parameters include φ_{cv}, φ_{p}, and *c*, and the densification parameters are *Rf*, f_{dens}, and f_{Post}.. these parameters are defined in Table 1.

FEM for sabkha soil

After selecting an appropriate constitutive model that captures the behavior of the considered soil, it is important to carefully evaluate the parameter used in the constitutive model to ensure accuracy. In this study, the strength parameters were set as the strength of the natural sabkha soil (Alnuaim et al., 2020). The monotonic and cyclic behavior of the soil at effective stresses of 50, 100, and 150 kPa have been studied by Alnuaim et al. (Alnuaim et al., 2020). They evaluated stiffness parameters of 18700, 20200, and 20300 kPa, which were employed as input data in this study. The K_B^e, K_G^e K_G^e, n_p, and R_f parameters were fine-tuned to enhance the FEA results compared to the experimental test in terms of stress-strain at different effective confining stresses (50, 100, and 150 kPa). Notably, m_e and n_e were initially set as 0.5. Fig. 1 shows the $q-\varepsilon_1$ curves obtained from FEM analysis and experimental tests at effective stress (σ_3') of 50 kPa, and they show good agreement. The densification parameters f_{dens} and f_{post} were adjusted to enhance the numerical results for the increase in excess PWP with the number of cyclic compared with the experimental results. Fig. 2 compares the FEM and experimental results of excess PWP with *N* for effective stress of 50 kPa. UBC3D-PLM showed high excess PWP in the first cycle. The main limitation of the UBC3D-PLM model is that it cannot consider the anisotropic consolidation effect during primary loading, which results in higher values of excess PWP during the first complete cycle (Petalas and Galavi, 2013).

Stiffness in the UBC3D-PLM model is stress-dependent and varies with depth. To accurately estimate the stiffness of natural sabkha soil at different stress levels, natural sabkha soil was divided horizontally into three layers (layer-1, -2, and -3), and the thicknesses of the layers were computed. The effective stress at the middle of layer-1, -2, and -3 were 50, 100, and 150 kPa, respectively. UBC3D-PLM parameters for the three layers are listed in Table 1. Notably, effective

stress includes the weight of the soil and induced stress from structures. An approximate method was used to compute the induced stress of the soil structure (Budhu, 2015).

Table 1 UBC3D-PLM parameters of the natural sabkha soil

Items	Define item	Layer-1	Layer-2	Layer-3
K_B^e	Elastic bulk modulus	150	190.5	100
K_G^e	Elastic shear modulus	80	90	54
K_G^p	Plastic shear modulus	800	275	350
me	Elastic shear modulus index	0.5	0.5	0.5
ne	Elastic bulk modulus index	0.5	0.5	0.5
np	Plastic shear modulus index	0.3	0.5	0.8
φ_{cv}	Constant volume friction angle	33	33	33
φ_p	Peak friction angle	33	33	33
c	Cohesion	9	9	4
N_{60}	SPT value	5	5	5
f_{dens}	Densification factor	0.3	6	0.6
f_{post}	Post liquefaction factor	0.7	12	0.8
σ_t	Tension cut-off	0	0	0
R_f	Failure ratio	0.9	0.94	0.91
Start level (m)		0	-8.5	-11.5
End level (m)		-8.5	-11.5	-25
σ_3' at mid layer (kPa)		50	100	>150

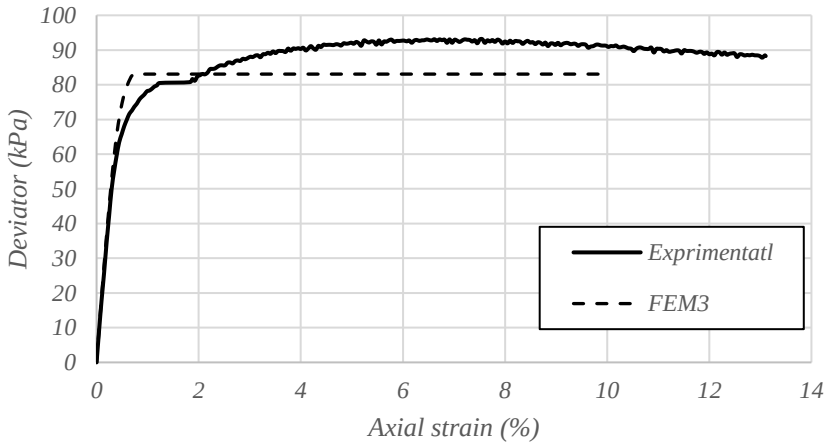

Fig. 1: Stress-strain for experimental and FEM for effective stress of 50 kPa

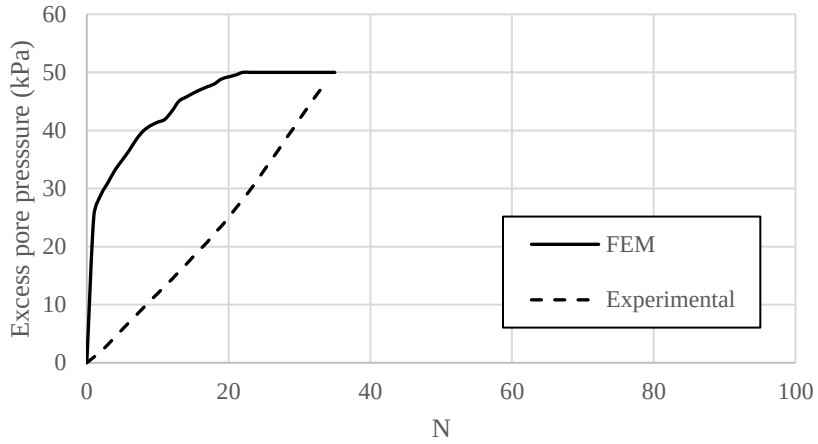

Fig 2: Excess PWP-N for experimental and FEM for effective stress of 50 kPa and *CSR* of 0.35

Parametric study

The effects of the vertical displacement amplitude, frequency, and foundation mass on the liquefaction behavior of the saturated salt-encrusted flat soil were investigated. In addition, the influence of the cement-stabilized sabkha layer underneath the vibrating foundation on the liquefaction potential was examined. Vertical displacement amplitudes were considered based on the maximum limit of amplitude vibration in machine performance and human tolerance. Based on the Baxter and Bernhart chart, which shows the permissible vibration for machine performance (Fig. 3 (a)), the boundary separated between “Slightly Rough” and “Rough regions” was marked (blue line), and the displacement amplitudes corresponding to operating frequencies of 5, 20, and 80 Hz were 0.5, 0.127, and 0.035 mm, respectively. Similarly, for human tolerance, the boundary edge between "Troublesome to person" and "Severe to person" regions was labeled (blue line) as shown in Fig 3 (b), and the displacement amplitudes corresponding to frequencies of 5, 20, and 80 Hz were 0.4, 0.04, and 0.004 mm, respectively. The lower bounds of the displacement amplitude were considered as 0.4, 0.04, and 0.004 mm.

The minimum frequency considered in the FEM analysis depends on the subsoil condition and geometry foundation as shown in Eq (3):

$$f_{min} = \frac{1}{2\pi r}\sqrt{\frac{G}{\rho}}, \qquad (3)$$

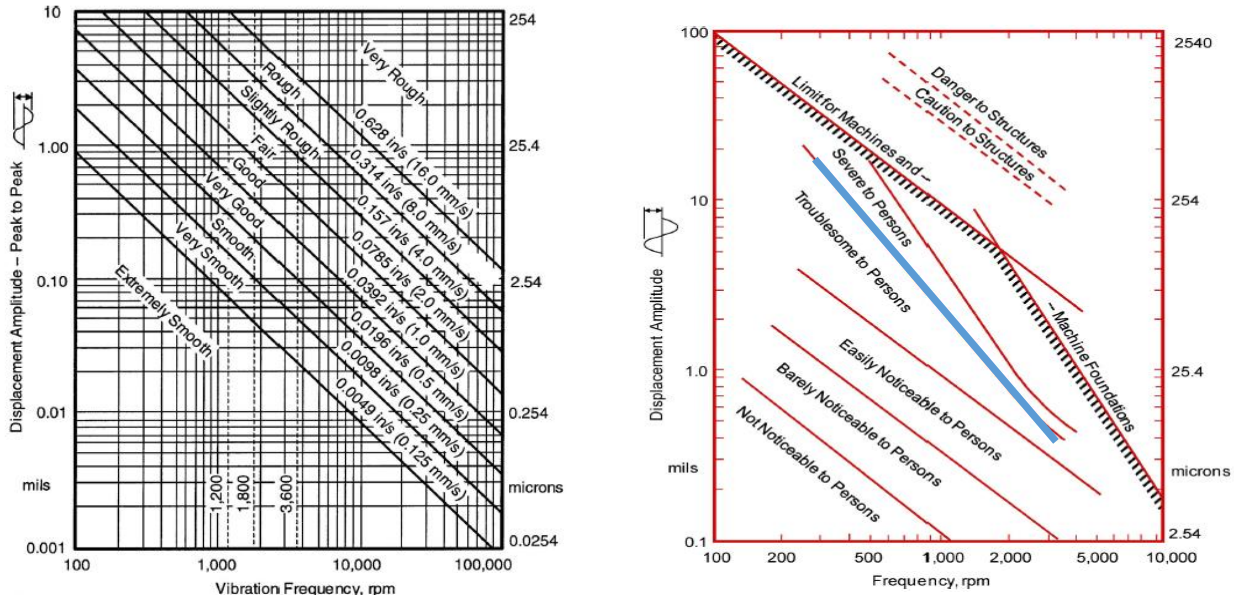

(a) (b)

Fig. 3**:** Machine vibration charts; (a) Baxter and Bernhart chart for machine performance; (b) Reiher–Meister chart for human tolerance.

where G and ρ are the shear modulus and density of the subsoil, respectively, and r is the foundation radius. The minimum frequency is 5 Hz when G, ρ, and r equal 10000 kPa, 1.51 t/m^3, and 2.5 m, respectively. The other two frequencies were set at 20 and 80 Hz, to cover the frequency used in practice.

The modified mass ratio ($B_v = \frac{1-\mu}{4}\frac{m}{\rho r^3}$) was computed to investigate the influence of the foundation mass on the liquefaction potential. It can be computed, μ and m are the Poisson ratio of the subsoil and the foundation mass, respectively. Because the subsoil is saturated, and the condition is undrained, a Poisson ratio of 0.45 (close to 0.5) was considered. The modified mass ratios were set as 0.001, 0.05, 0.12, and 0.23, corresponding to the foundation thicknesses of 0.01, 0.1, 0.3, and 0.6 m, respectively. Notably, B_v of 0.001 indicates a massless foundation. cement

content percentages (5 and 10%) were considered to treat the sabkha layer. Furthermore, the thickness of the treated sabkha layer was set as 0.12, 0.24, and 0.48 times the foundation diameter.

RESULTS AND DISCUSSIONS

To examine the liquefaction of sabkha under massless or mass vibrating foundations the PWP ratio (r_u) at different levels in the natural sabkha profile was evaluated. (r_u) is defined as the ratio of excess PWP at a given dynamic time to the initial effective stress (effective stress at the start of vibration loading). Figure 4 shows the effective stress history at a depth of 0.5 m under the massless foundation that rested immediately on the natural sabkha for frequency and displacement amplitude of 80 Hz and 0.04 mm, respectively. The effective stress reaches zero (liquefied) after a few cycles (6th cycle). Figure 5 shows the effect of the frequency of a vibrating foundation on r_u at different depths below the centerline of the foundation. The PWP ratio equals unity just underneath the foundation, and it decreases with depth. The liquefied zone (the zone at which r_u equals unity) starts at the base of the foundation and increases with operating frequenc

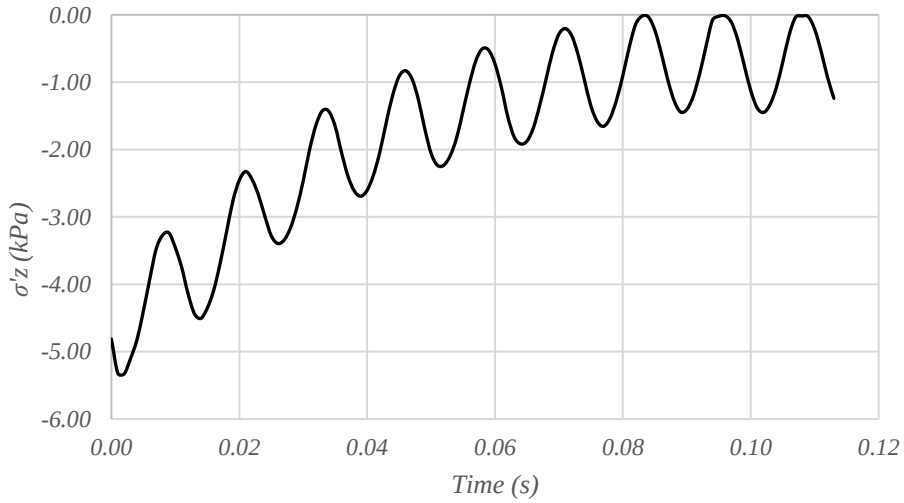

Fig. 4**:** Time history of effective stress (σ_z') at a depth 0.5 m below the vibration foundation at the operating frequency of 80 Hz.

Figure 12 shows a typical change in PWP ratio with depth along the centerline for different B_v. The induced displacement amplitude and operating frequencies were 0.04 mm and 20 Hz, respectively. The largest increment of PWP is observed at a point just below the foundation. The PWP ratio r_u generally decreases with depth because an increase in the effective stress induced by the weight of soil with a depth decreases r_u. Beaty and Perlea (Beaty & Perlea, 2011) considered zones with a maximum r_u greater than 0.7 to be liquefied. Fig. 6 shows that, at a foundation level, B_v of 0.0028 and 0.058 corresponds to maximum r_u of 1.0 and 0.74, respectively. However, the maximum pore pressure ratio for B_v of 0.17 and 0.3 are approximately 0.43 and 0.36, respectively, which indicates a non-liquefiable condition. The foundation mass has two effects (positive and negative effects). The positive effect of foundation mass is the increase in the effective stress of sabkha soil particles and the decrease in the value of r_u by at least 0.3. On the other hand, the negative effect is that the inertia forces of the foundation increase the value of r_u; however, based on the results of FEM, the inertia forces may have a minimal effect. In addition, by interpolating the value B_v and the corresponding value of r_u, the mass ratio that initiates liquefaction is 0.1445 during a 5-s operation. Therefore, the minimum mass ratio required to prevent the liquefaction at a dimensionless frequency (α) of less than 9.96 is 0.1445. The dimensionless frequency depends on the angular frequency (ω), r the foundation radius (r), and the subsoil condition in terms of density (ρ) and shear modulus (G). It was represented as [$\alpha = \omega r\sqrt{(\rho \,/\, G)}$]. In other words, the minimum foundation mass that prevents liquefaction in the sabkha soil depends on the ratio of the machine's velocity to the shear wave velocity of the subsoil (sabkha).

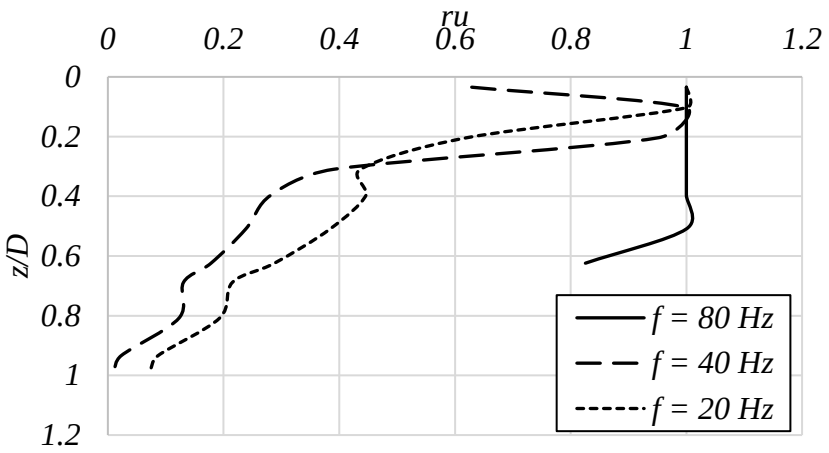

Fig. 5: PWP ratio with depth under massless vibration foundation at several frequencies at t = 5 sec, under displacement amplitude A_z = 0.04 mm.

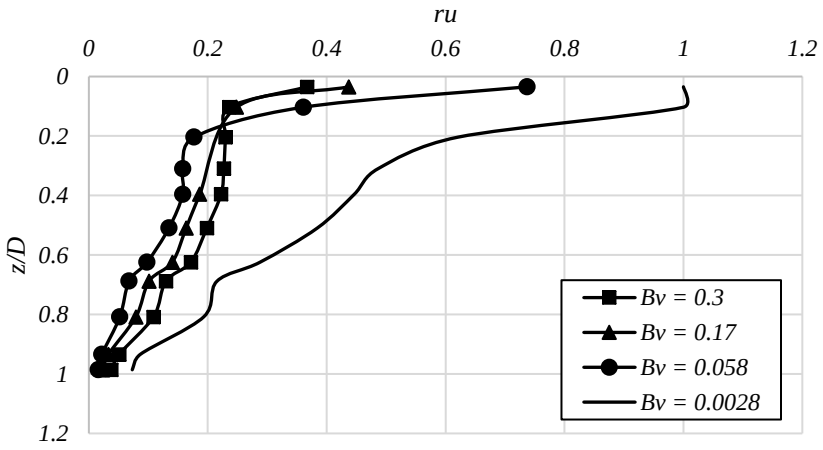

Fig. 6: Influence of foundation's mass on PWP ratio.

The numerical and experimental studies that were carried out by Fattah et al 2015 and Fattah et al 2017 on shallow foundations that rested on saturated soil and were subjected to vertical harmonic loading with different frequencies showed that there was no liquefaction in the supported saturated sand. These results agreed with the results of this paper in terms of mass foundation rested on the saturated sabkha soil. It is important to identify the limitation of the study and there were four limitations in this study to simplify the analysis: (1) the type of machine foundation is a

block foundation; (2) the subsoil is saturated sabkha soil; (3) the embedment depth is zero; and (4) the cross-section shape of the foundation is circular with a diameter of 5 m.

CONCLUSIONS

In this study, the effect of a machine foundation that has a vertical vibration loading on the liquefaction potential of sabkha soil (subsoil) was investigated using numerical analysis. The parameters studied include vertical displacement amplitude (400, 40, and 4 μm), frequency (5, 20, and 80 Hz), foundation mass modified mass ratio of foundation (Bv = 0.0028, 0.058, 0.17, and 0.3). The sabkha soil was modeled using the UBC-PLM constitutive model based on the static and dynamic properties of the soil. While the circular foundation was modeled as linear elastic concrete material, the foundation's diameter was kept constant at 5 m. The dynamic issues of modeling in terms of element size, time increment, and viscous boundary conditions were considered. The pore water pressure (PWP) ratio (r_u) which is defined as the ratio of pore water pressure to the initial effective stress of points at different levels in the natural sabkha soil profile under a vibrating foundation was evaluated. The main finding revealed that r_u increases with depth and then decreases. The operating frequency of vertical vibration loading increases PWP. For massless foundation (Bv = 0.0028, massless foundation) and foundation with a thickness of 0.15 m (Bv = 0.058), liquefaction was observed in the sabkha soil at a depth close to the subsurface, and the corresponding maximum r_u was 1.00 and 0.74, respectively. The variation in r_u in the sabkha increases with decreasing foundation mass.

Acknowledgments

The authors would like to acknowledge the Researchers Supporting Project number (RSP-2021/285), King Saud University, Riyadh, Saudi Arabia.

Funding

Researchers Supporting Project number (RSP-2021/285), King Saud University, Riyadh, Saudi Arabia.

REFERENCES

Ahmed, H. R. & Al Shayea, N. A. 2017. Seismic behavior and zoning of the sabkha soils in Jubail industrial city, Saudi Arabia. *Journal of Seismology*. https://doi.org/10.1007/s10950-017-9657-1

Al-Amoudi, O. S. B. & Abduljauwad, S. N. 1994. Modified odometer for arid, saline soils. *Journal of Geotechnical Engineering*, *120*(10), 1892–1897.

Al-Amoudi, O. S. B. & Abduljauwad, S. N. 1995. Compressibility and collapse characteristics of arid saline sabkha soils. *Engineering Geology*. https://doi.org/10.1016/0013-7952(95)00016-9

Al-Shamrani, M. A. 2004. Applicability of the rectangular hyperbolic method to settlement predictions of sabkha soils. *Geotechnical and Geological Engineering*. https://doi.org/10.1023/B:GEGE.0000047046.73649.04

Al-Shamrani, M. A. & Dhowian, A. W. 1996. Characterization of secondary compression behavior of Sabkhasoils. *Engineering Geology*.

A**lnuaim, A., Alsanabani, N. & Alshenawy, A. 2020**. Monotonic and Cyclic Behavior of Salt-Encrusted Flat (Sabkha) Soil. *International Journal of Civil Engineering*, 1–12.

A**mini, F. & Qi, G. Z. 2000**. Liquefaction testing of stratified silty sands. *Journal of Geotechnical and Geoenvironmental Engineering*, *126*(3), 208–217.

ASTM D2216-10. 2010. Standard test methods for laboratory determination of water (Moisture) Content of Soil and Rock by Mass 1. *ASTM International*. https://doi.org/10.1520/D2216-10

ASTM D422. 2007. Standard test method for particle-size analysis of soils. *ASTM International*. https://doi.org/10.1520/D0422-63R07E02

ASTM D4318-10. 2010. Standard test methods for liquid limit, plastic limit, and plasticity index of soils. *ASTM International*. https://doi.org/10.1520/D4318-10

ASTM D6938–10. 2010. Standard test method for in place density and water content of soil and soil aggregate by nuclear methods (Shallow Depth). *ASTM International*. https://doi.org/10.1520/D6938-10

ASTM D854. 2010. Standard test for specific gravity of soil solids by water pycnometer. In *ASTM International*. https://doi.org/10.1520/D0854-10

Bathe, K.-J. 2006. *Finite element procedures*. Klaus-Jurgen Bathe.

Beaty, M. H. & Perlea, V. G. 2011. Several observations on advanced analyses with liquefiable materials. *Proceedings of the 31st Annual USSD Conference and 21st Conference on Century Dam Design-Advances and Adaptations*, 1369–1397.

Bhatia, K. G. 2008. Foundations for industrial machines and earthquake effects. *ISET Journal of Earthquake Technology*, *45*(1–2), 13–29.

Budhu, M. 2015. Soil Mechanics Fundamentals. John Wiley & Sons.

El Fiky, N. E., Metwally, K. G. & Akl, A. Y. 2020. Effect of top soil liquefaction potential on the seismic response of the embedded piles. *Ain Shams Engineering Journal*, *11*(4), 923–931.

Fattah, M. Y., Al-Mosawi, M. J., & Al-Americ, A. F. I. 2017. Stresses and pore water pressure induced by machine foundation on saturated sand. *Ocean Engineering*, *146*, 268–281.

Fattah, M. Y., Salim, N. M., & Al-Shammary, W. T. 2015. Effect of embedment depth on response of machine foundation on saturated sand. *Arabian Journal for Science and Engineering*, *40*(11), 3075–3098.

Ibrahim, K. M. H. I. 2014. Liquefaction analysis of alluvial soil deposits in Bedsa southwest of Cairo. *Ain Shams Engineering Journal*, *5*(3), 647–655.

Kramer, S. L. 1996. Geotechnical earthquake engineering. Pearson Education India.

Lee, C. Y. 2007. Earthquake-induced settlements in saturated sandy soils. *ARPN Journal of Engineering and Applied Sciences*, *2*(4), 6–13.

Mokhtar, A.-S. A., Abdel-Motaal, M. A. & Wahidy, M. M. 2014. Lateral displacement and pile instability due to soil liquefaction using numerical model. *Ain Shams Engineering Journal*, *5*(4), 1019–1032.

MUÑOZ, B. O. M. **2008**. Plaxis version 8 dynamics manual.

Petalas, A. & Galavi, V. 2013. Plaxis liquefaction model ubc3d-plm. *Plaxis Report*.

Rollins, K. M. & Seed, H. B. 1990. Influence of buildings on potential liquefaction damage. *Journal of Geotechnical Engineering*, *116*(2), 165–185.

Seed, H. B., Idriss, I. M., & Arango, I. 1983. Evaluation of liquefaction potential using field performance data. *Journal of Geotechnical Engineering*, *109*(3), 458–482.

Vaid, Y. P. & Thomas, J. 1995. Liquefaction and postliquefaction behavior of sand. *Journal of Geotechnical Engineering*, *121*(2), 163–173.

Yoshimi, Y. 1967. An experimental study of liquefaction of saturated sands. *Soils and Foundations*, *7*(2), 20–32.

Zeghal, M. & Elgamal, A.-W. **1994**. Analysis of site liquefaction using earthquake records. *Journal of Geotechnical Engineering*, *120*(6), 996–1017.